Journal Pre-proof

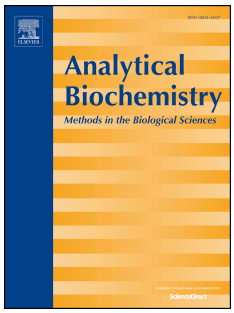

A sensitive H_2O_2 biosensor based on carbon nanotubes/tetrathiafulvalene and its application in detecting NADH

Xingcan Huang, Jiru Zhang, Lili Zhang, Hang Su, Xiumei Liu, Jian Liu

PII: S0003-2697(19)30650-5

DOI: https://doi.org/10.1016/j.ab.2019.113493

Reference: YABIO 113493

To appear in: *Analytical Biochemistry*

Received Date: 5 July 2019

Revised Date: 12 October 2019

Accepted Date: 29 October 2019

Please cite this article as: X. Huang, J. Zhang, L. Zhang, H. Su, X. Liu, J. Liu, A sensitive H_2O_2 biosensor based on carbon nanotubes/tetrathiafulvalene and its application in detecting NADH, *Analytical Biochemistry* (2019), doi: https://doi.org/10.1016/j.ab.2019.113493.

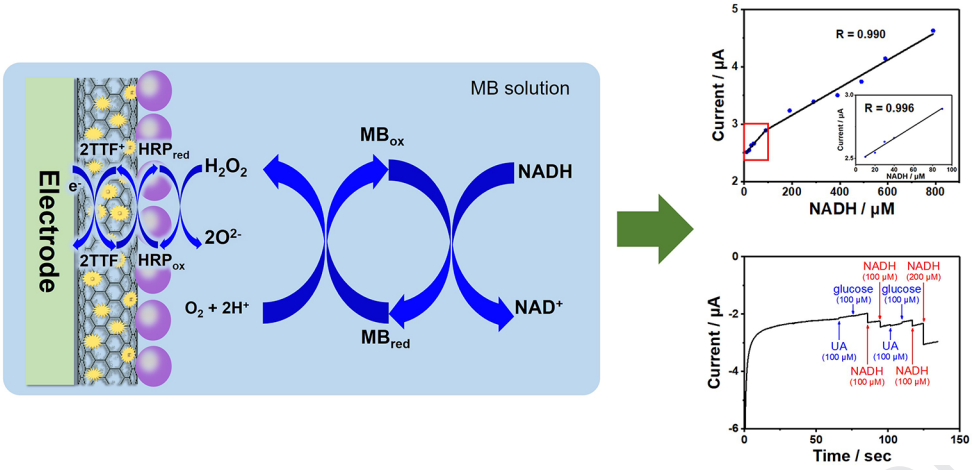

A sensitive H_2O_2 biosensor based on carbon nanotubes/tetrathiafulvalene and its application in detecting NADH

Xingcan Huang [a, §], Jiru Zhang [a, §], Lili Zhang[b, *], Hang Su[a], Xiumei Liu[c], Jian Liu[a, *]

[a] *School of Control Science and Engineering, Shandong University, Jinan, 250061, China*

[b] *School of Mechanical and Automotive Engineering, Qilu University of Technology, Jinan, 250353, China*

[c] *School of Pharmaceutical Sciences, Shandong University, Jinan 250012, China*

[§] *These authors contributed equally to this work*

**Corresponding author: J. Liu: lj@sdu.edu.cn; L.Zhang: sdilizll@163.com*

Abstract

Reduced nicotinamide adenine dinucleotide (NADH) plays a pivotal role in the electron-transfer chain of biological system. Analysis of many biological markers is based on the detection of the enzymatically generated NADH. In this paper, a sensitive hydrogen peroxide (H_2O_2) biosensor, fabricated by carbon nanotubes (CNTs)/tetrathiafulvalene (TTF)/horseradish peroxidase (HRP), was applied for detecting the NADH in a buffer containing methylene blue (MB) at low operating potential of - 0.3 V (*vs.* Ag/AgCl). Since the NADH could be oxidized by MB to release H_2O_2, the electrochemical biosensor enables to detect the NADH in the MB buffer. And the low working potential made the biosensor avoid the interference from other electroactive substances. Linear response ranges from 10 μM to 790 μM, with a sensitivity of 4.76 μA mM^{-1} and a detection limit of 1.53 μM were obtained under the optimum conditions. The proposed sensor provided a promising approach for sensitively detecting the NADH.

Keyword: modified electrode, carbon nanotubes, hydrogen peroxide, biosensor, NADH

1. Introduction

It is generally known that the reduced nicotinamide adenine dinucleotide (NADH) and its oxidized form, nicotinamide adenine dinucleotide (NAD^+), are very common and important biomolecules in the living cells. As a pair of enzyme cofactors, the redox couple NADH/ NAD^+ play an essential part in the process of complex enzymatic reactions of more than 300 dehydrogenases [1, 2]. Besides, the NADH/NAD^+ coenzymes have been widely used in the application of enzyme activity assays for the diagnosis of diseases such as ischemia and neoplasia [3], as well as the study of dehydrogenase-based biosensors and biofuel cells [4, 5]. And some scientists have found that NADH is beneficial for the therapy of Parkinson's disease, Alzheimer's disease, and depression etc

[6, 7]. Thus, developing high accuracy approaches to detect the concentration of NADH has attracted extensive attention.

Nevertheless, the direct electrochemical oxidation of NADH to NAD^+ at a bare solid electrode is slow and highly irreversible. And the reaction proceeds only at high overpotentials accompanying with the side products of methyl, propyl and benzyl reactants that would strongly adsorb onto the electrode surface [8-10]. Recently, some technologies for detecting NADH have been developed, including chemiluminescence [11], photoelectrochemistry [12], electrochemiluminescence [13], colorimetry [14] and electrochemical assay [10, 15]. Thereinto, electrochemical approaches would be the most prospective way due to their high specificity, rapid response and straightforward operation [10]. The amperometric detection method for determining NADH has been studied previously based on the employment of methylene blue (MB) [3] or 5-methylphenazinium methosulfate as electron mediators [9]. It is well known that the oxidized MB can react with NADH, and the resulting reduced MB then reacts with O_2 to produce hydrogen peroxide (H_2O_2) (Eq. (1-2)) [11].

$$H^+ + NADH + MB_{oxidized} \rightarrow NAD^+ + MB_{reduced} \quad (1)$$

$$MB_{reduced} + O_2 \rightarrow MB_{oxidized} + H_2O_2 \quad (2)$$

However, due to the good water-soluble of MB, there are some difficulties in immobilizing method for preventing from the loss of mediators [3]. According to the equations, it is feasible to determine the amount of NADH through indirect detection of H_2O_2 in the aqueous solution containing MB. More importantly, H_2O_2 probes are always allowed to work at a relatively low operating voltage [16, 17], which could overcome the bottlenecks of high overpotentials and avoid the interference from some common electroactive substances.

In this paper, a novel H_2O_2 biosensor is fabricated for detecting the concentration of NADH. The biosensor was fabricated by casting the carbon nanotubes (CNTs)/tetrathiafulvalene (TTF) composite substrate and horseradish peroxidase (HRP) on the electrode. The composite of CNTs/TTF was simply fabricated according to the solubility of TTF in ethanol solution. Because of the combination of carbon-based nanomaterial and mediator, biosensors based on the hybrid would show excellent conductivity and electron transfer. Besides, the manufacturing cost of this hybrid is much lower than the hybridization of carbon materials and noble metals [18, 19]. In order to achieve the sensitive detection of NADH, the water-soluble MB is dissolved in an aqueous solution instead of directly modified on the electrode, as shown in Fig. 1. Under the optimum working voltage, the amperometric detection method of NADH using the assembled H_2O_2 biosensor has characteristics of simple preparation, good stability, high sensitivity and low detection limit.

Fig. 1.

2. Experimental

2.1 Reagents

Horseradish peroxidase (HRP, Type VI, ≥250 units/mg solid), tetrathiafulvalene (TTF, 97%),

bovine serum albumin (BSA, ≥98%), carbon nanotubes (CNTs, >8% carboxylic acid functionalized), glutaraldehyde solution (GA, 25 wt% in water), chitosan (medium molecular weight), reduced nicotinamide adenine dinucleotide (NADH, ≥97%), methylene blue (MB), hydrogen peroxide solution (H_2O_2, 3 wt% in H_2O) and phosphate buffer saline (PBS, pH 7.4) were purchased from Sigma-Aldrich. All chemicals used in the study were analytical reagent grade and without further purification. And all aqueous solutions were prepared with ultrapure water (>18 MΩ cm).

2.2 Apparatus

Surface topography and structure characterizations were obtained by a JSM-7800F field emission scanning electron microscope (SEM, JEOL Ltd., Japan) operating at 3 kV. All electrochemical measurements including cyclic voltammetry (CV), electrochemical impedance spectroscopy (EIS) and amperometric measurments were carried out in a conventional three-electrode system controlled by the electrochemical work station of CHI 660E (CH Instruments, USA). The modified glass carbon (GC, 5 mm in diameter) electrode was used as the working electrode. The platinum (Pt) wire and Ag/AgCl (soaked in 3 M KCl) were selected as the counter electrode and reference electrode, respectively. The amperometric measurements and CV curves were carried out in the 0.1 M PBS solution containing different concentration sample, and the response current was acquired by comparing the change value between the steady-state current and background current. In addition, the EIS was taken in the solution of 5 mM $K_4Fe(CN)_6/K_3Fe(CN)_6$ within a frequency range of 100 kHz to 1 Hz.

2.3 Preparation of CNTs/TTF/HRP Modified Electrode

Before the modification, GC electrode was successive polished by 0.3 μm and 0.05 μm alumina slurry and dried for 2 hours. The mixture solution of CNTs and TTF was obtained by adding 1.5 g CNTs into 1 mL 0.05 M TTF ethanol solution and immersed for 24 hours. Next, 2 μL mixture solution were dropped onto the surface of pretreated GC electrode and dried at the room temperature. Here, the CNTs/TTF composite modified electrode was obtained by the precipitation of TTF on the sidewalls of CNTs. For comparison, GC/CNTs and GC/CNTs/TTF electrodes were also prepared with the same procedure.

For the fabrication of HRP-based enzyme electrode, the catalytic ink was firstly prepared by blending 1 μL HRP (4 U/μL) and 1 μL BSA (10 mg mL^{-1}). Then the adsorbed CNTs/TTF film electrode was subsequently coated with the biocatalytic HRP layer and stored at 4 °C refrigerator for 1 hour. Following this, 2 μL GA (5 wt%) and 2 μL chitosan was dropped onto the surface of CNTs/TTF/HRP sensitive film in order to improve the stability of fabricated biosensor. Then, the electrode was allowed to dry at 4 °C refrigerator for overnight. Regarding the reversibility and stability test of the biosensor, detailed explanations are in the SI section.

3. Results and discussion

3.1 Characterization and electrochemical analysis

In this work, a simple method was introduced to immobilize CNTs/TTF composite on the electrode as electron transfer shuttle between HRP active center and electrode surface. The modified electrode of CNTs/TTF/HRP was expected to maintain the electrocatalytic properties of HRP and have ability to detect low concentration of H_2O_2. And the H_2O_2 biosensor would be further used to study the ectrocatalytic oxidation of NADH in the presence of MB. Prior to the reactions, various composites were characterized by CV, EIS and SEM to research their electrochemical and structure properties.

Fig. 2A showed the SEM image of CNTs, which was found obvious stereoscopic tubular structure with large specific surface area. As shown in Fig. 2B that the TTF was densely attached on the sidewalls of CNTs to build the CNTs/TTF composite structure. Combining CNTs with TTF could not only facilitate the electron transfer between enzyme activity center and electrode surface, but also increase the amount of immobilized enzymes because of their three-dimensional reticulated space structure, and then improve the performance of biosensors.

Fig. 2.

Additionally, EIS measurements achieved in the $Fe(CN)_6^{4-}/Fe(CN)_6^{3-}$ solution were chosen to further confirm the immobilization of TTF and HRP, in that the results were able to demonstrate the electrolyte/charge transfer resistances (R_s/R_{ct}) of corresponding electrodes. Fig. 3A displayed the fitting curves of EIS tests about different electrodes. According to Nyquist plots, the intercepts of semicircles represented the R_s value which was determined by the test solution, and the diameters of the semicircles reflected the R_{ct} that was straightly associated with the modified compounds on electrodes. It could be observed that the R_s values of all electrodes were similar (about 50 Ω) because of the same electrolyte. On the contrary, the R_{ct} of different electrodes varied greatly based on the difference of modified materials. Among them, the R_{ct} value of bare GC electrode was fitted as 29.3 Ω which was higher than that of 15.5 Ω for GC/CNTs electrode (curve b), indicating the CNTs could act as the good electron transfer interface between the EIS probe and the electrode. Besides, because of the successful immobilization of TTF on the surface of CNTs, the curve c showed larger diameter of 39.62 Ω. Furthermore, the largest R_{ct} of 108.1 Ω for GC/CNTs/TTF/HRP (curve d) directly indicated the presence of HRP, in that enzymes were non-conductive and hindered the redox probe's access to the electrode surface [20].

The electrochemical performance of GC/CNTs/TTF/HRP electrode was investigated by CV curves measured in the 0.1 M PBS solution saturated with N_2 at a scan rate of 100mV s^{-1}. The results of bare GC electrode (curve a), a GC/CNTs electrode (curve b), a GC/CNTs/TTF electrode (curve c) and GC/CNTs/TTF/HRP modified GC electrode (curve d) were all shown in Fig. 3B. Obviously, in comparison to other electrodes without HRP, the GC/CNTs/TTF/HRP electrode showed a pair of stable and well-defined redox peaks, which could be ascribed to the electron transfer between the HRP and electrode substrate [21]. And the anodic peak potential (E_{pa}) and cathodic peak potential (E_{pc}) were located at - 0.28 V and - 0.17 V *vs.* Ag/AgCl, respectively. Moreover, Fig. 3C showed the CV curves of GC/CNTs/TTF/HRP electrode in the 0.1 M PBS solution at the scan rate from 10 mV

s^{-1} to 100 mV s^{-1}. It could be seen that the redox peak potential was almost unchanged with the increasing scan rate, while there were corresponding increases in both oxidation and reduction peak currents. There was also a linear proportionality between redox peak current and scan rate, as shown in Fig. 3D. Furthermore, it was clear that the value of oxidation peak current were almost as large as that of reduction peak under the same scan rates, demonstrating the redox progress of HRP immobilized on the CNTs/TTF electrode substrate was reversible and surface-controlled. As a result, the CNTs/TTF modified electrode could lead to more HRP molecules loading and rapid electron transfer rate between the active center of enzyme and electrode. On the one hand, CNTs have the properties of porous structure, high electrical conductivity good biocompatibility and large surface area [22-25]. On the other hand, TTF as the electron transfer mediator yields lower oxidation potential and lower toxicity than ferrocene derivatives, Meldola blue etc [26]. Coupling with the high solubility of TTF in the ethanol, the TTF can straightforwardly separate out on the sidewalls of CNTs with the volatilization of ethanol in mixture solution to form CNTs/TTF composite. Thus, the CNTs/TTF composite would have promising application in the field of biosensors.

Fig. 3.

3.2 Detection of H_2O_2 on GC/CNTs/TTF/HRP electrode

Electrocatalytical activity of enzyme electrode was firstly study by CV test in the 0.1 M PBS buffer with different concentration of H_2O_2. Fig. 4A exhibited the results in the absence (curve a) and in the presence of increasing H_2O_2 concentration (curves b-d) at a scan rate of 100 mV s^{-1}. It was obvious that well-defined redox peaks of H_2O_2 were obtained and the reduction peak currents increased dramatically upon the addition of H_2O_2, which was a typical representation of the catalytic reduction of H_2O_2. This indicated that the GC/CNTs/TTF/HRP electrode showed excellent electrocatalytical activity for H_2O_2. The reaction mechanism of the immobilized HRP towards H_2O_2 could be interpreted by the following cycles [27, 28]:

$$HRP + H_2O_2 \rightarrow Compound\ \ I + H_2O \quad (3)$$

$$Compound\ \ I + e^- \rightarrow Compound\ \ II \quad (4)$$

$$Compound\ \ II + e^- \rightarrow HRP \quad (5)$$

HRP is oxidized to the first intermediate (Compound Ⅰ) via the reaction with H_2O_2. Compound Ⅰ shows catalytic activity, and then obtains one electron from the electrode to form a second intermediate (Compound Ⅱ). Subsequently, Compound Ⅱ is reduced to HRP by accepting another electron from electrodes. Hence, the reduction current will increase in the presence of H_2O_2. [26] It could be seen that the reduction of H_2O_2 started at negative potentials and reached a maximum at about - 0.3 V *vs.* Ag/AgCl, indicating that the GC/CNTs/TTF/HRP electrode had a low working potential for monitoring the reduction of H_2O_2. Because background currents influenced readings, the operation of the sensor at low potential was analytically desirable to reduce the electrochemical interferences and achieve high selectivity; therefore, a low operating potential of - 0.3 V was chosen

to demonstrate the applicability of this biosensor for detecting H_2O_2.

Furthermore, amperometric i–t curve is the regularly utilized technique to assess the detection limits and linear ranges of electrochemical sensors. The amperometric responses of the assembled sensor were investigated by successive dropping H_2O_2 into PBS buffer with an operating potential of - 0.3 V, as shown in Fig. 4B. It was clear that the response current increased with the addition of H_2O_2, and the time of reaching steady-state current platform was short which demonstrated that the biosensor possessed the quick response to the target molecule. The calibration curve showed linear relationship of response current versus the concentration of H_2O_2 in a large concentrations ranging from 100 μM to 350 mM with a correlation coefficient of 0.996 (n=16) (Fig. 4C). From the slope of the resulting curve, a detection limit of 10 μM was estimated at a signal-to-noise ratio of 3 (S/N=3). Besides, the Michaelis–Menten constant (K_m) provides an indication of the enzyme–substrate kinetics and is generally used to evaluate the biological activity of the immobilized enzyme [29]. According to the Lineweaver–Burk equation, the K_m of the GC/CNTs/TTF/HRP electrode was calculated as 0.49 mM, which was lower than other H_2O_2 sensors [30-33]. In short, the biosensor displayed high sensitivity accompanied by a low noise level, allowing convenient detection of micromolor concentrations and thus creating conditions for the further detection of NADH.

Fig. 4.

3.3 Determination of NADH with H_2O_2 biosensor

According to Eq. (1-2), the MB has ability to oxidize NADH at the same time transforming to its reduction state, and then the reduced MB could react with O_2 to produce H_2O_2. Hence, determining the concentration of NADH through H_2O_2 biosensors is a novel way to avoid high working potential and improve anti-interference ability and detecting accuracy.

Similarly, CV and amperometric i–t curve were utilized to evaluate the effect for detecting NADH through CNTs/TTF/HRP sensitive thin film modified H_2O_2 biosensor. In the 0.1 M PBS solution that containing 0.5mM MB, the oxidation peak current and reduction peak current both increased with the addition of NADH (0-0.6 mM), which was exhibited in Fig. 5A. That is to say, NADH is firstly oxidized to NAD^+ by MB when it is added into the solution; as a result the oxidation current rise up. Then, the reduction of O_2 occur in the presence of the reduced MB; at the same time, H_2O_2 is produced and the reduction current increase. Although there were peak potential shifts that may caused by the presentence of MB, little negative influences occurred for electrocatalytical activity of the biosensor. Moreover, Fig. 5B demonstrated the amperometric responses with successive injection of NADH into the background solution under an applied potential of - 0.3 V. The current of the enzyme electrode increased with the addition of NADH and rapidly reached a steady state, indicating the practicability of determining NADH through H_2O_2 biosensor in the PBS solution with MB. Calibration curve that derived from amperometric data was shown in Fig. 5C. In this figure, two linear ranges were shown: one from 10 μM to 90 μM with a correlation coefficient of 0.996 and a sensitivity of 4.76 μA mM^{-1}, and the other from 90 μM to 790 μM with a correlation coefficient of 0.990 and a sensitivity of 2.4 μA mM^{-1}. And the detection limit was estimated as 1.53 μM (S/N=3). The reversibility of the proposed biosensor had been investigated, which demonstrated the excellent

performance of the H_2O_2 biosensor. As described in Fig. S1, the current values maintained 91% of its initial activity after five days at a specific concentration of NADH. Furthermore, Fig. S2 showed the current tendencies was stable by repeated measurements with the particular concentration gradient. In addition, to investigate the effect of some possible interfering matters for detecting NADH, the selectivity and anti-interference ability of the GC/CNTs/TTF/HRP electrode were evaluated by adding some interfering substances like uric acid (UA) and glucose. As exhibited in Fig. 5D, there was little current disturbance with successive addition UA and glucose, while the well-defined signal response could be obtained with different concentration of NADH as before. This result proved that interfering species had little effect for determining NADH at this working potential. And the fabricated biosensor displayed good anti-interference ability and selectivity. Comparing with other amperometric NADH biosensor in the Table 1, the H_2O_2 biosensor modified by CNTs/TTF/HRP sensitive film had excellent properties for determining the concentration of NADH with low operating potential, low detection limit, wide linear range as well as good anti-interference ability.

Fig. 5.

Table 1.

4. Conclusion

In this study, a H_2O_2 biosensor modified by the CNTs/TTF/HRP sensitive thin film was proposed to detect the concentration of NADH at a low operating potential of - 0.3 V. The fabricated CNTs/TTF composite exhibited three-dimensional reticulated space structure, leading to more HRP molecules loading and rapid electron transfer rate. The biosensor showed excellent electrocatalytic properties for H_2O_2 and provided a large linear concentration range of 100 μM to 350 mM as well as a detection limit of 10 μM. In the presence of MB, the response current for determining NADH was linearly proportional to the concentration of NADH in the range of 10 μM to 790 μM with a high sensitive of 4.76 μA mM^{-1} and a low detection limit of 1.53 μM (S/N=3). In addition, the low working potential made the biosensor overcome the high overpotentials for the oxidation of NADH and avoid the interference from other electroactive substances. The new strategy for detecting NADH in the presence of MB through CNTs/TTF/HRP modified H_2O_2 biosensor would have wide application prospects.

Conflicts of interest

Declarations of interest: none.

Acknowledgment

This work was supported by the National Natural Science Foundation of China (61801256, U1806202), Shandong Province Key Research and Development Plan (2018GGX109016) and Natural Science Foundation of Shandong Province (ZR2018ZC0129).

References:

[1] L. Gorton, E. Domínguez, Electrochemistry of NAD (P)+/NAD (P) H, Encyclopedia of Electrochemistry: Online. (2007)

[2] N. Li, G. Chen, Flow injection analysis of trace amounts of NADH with inhibited chemiluminescent detection, Talanta. 57 (2002) 961-967. http://doi.org/10.1016/S0039-9140(02)00125-X.

[3] E. Erçarıkcı, O. Bayındır, M. Alanyalıoğlu, Amperometric Quantification of NADH Based on Graphene/Methylene Blue Nanocomposite Thin Films on Au(111), Polym. Composite. 38 (2017) E118-E127. http://doi.org/10.1002/pc.24021.

[4] M. Hatada, N. Loew, Y. Inose-Takahashi, J. Okuda-Shimazaki, W. Tsugawa, A. Mulchandani, K. Sode, Development of a glucose sensor employing quick and easy modification method with mediator for altering electron acceptor preference, Bioelectrochemistry. 121 (2018) 185-190. http://doi.org/10.1016/j.bioelechem.2018.02.001.

[5] R. C. Reid, S. D. Minteer, B. K. Gale, Contact lens biofuel cell tested in a synthetic tear solution, Biosensors and Bioelectronics. 68 (2015) 142-148. http://doi.org/10.1016/j.bios.2014.12.034.

[6] R. Moradi, S. A. Sebt, H. Karimi-Maleh, R. Sadeghi, F. Karimi, A. Bahari, H. Arabi, Synthesis and application of FePt/CNTs nanocomposite as a sensor and novel amide ligand as a mediator for simultaneous determination of glutathione, nicotinamide adenine dinucleotide and tryptophan, Physical chemistry chemical physics : PCCP. 15 (2013) 5888-5897. http://doi.org/10.1039/c3cp00033h.

[7] S. Lin, L. Guarente, Nicotinamide adenine dinucleotide, a metabolic regulator of transcription, longevity and disease, Curr. Opin. Cell Biol. 15 (2003) 241-246. http://doi.org/10.1016/S0955-0674(03)00006-1.

[8] A. Radoi, D. Compagnone, Recent advances in NADH electrochemical sensing design, Bioelectrochemistry. 76 (2009) 126-134. http://doi.org/10.1016/j.bioelechem.2009.06.008.

[9] M. Vreeke, R. Maidan, A. Heller, Hydrogen peroxide and .beta.-nicotinamide adenine dinucleotide sensing amperometric electrodes based on electrical connection of horseradish peroxidase redox centers to electrodes through a three-dimensional electron relaying polymer network, Anal. Chem. 64 (1992) 3084-3090. http://doi.org/10.1021/ac00048a004.

[10] M. Govindhan, M. Amiri, A. Chen, Au nanoparticle/graphene nanocomposite as a platform for the sensitive detection of NADH in human urine, Biosensors and Bioelectronics. 66 (2015) 474-480. http://doi.org/10.1016/j.bios.2014.12.012.

[11] D. R. Williams, W. R. Seitz, Automated chemiluminescence method for determining the reduced form of nicotinamide adenine dinucleotide coupled to the measurement of lactate dehydrogenase activity, Anal. Chem. 48 (1976) 1478-1481.

[12] Y. Dilgin, D. G. Dilgin, Z. Dursun, H. İ. Gökçel, D. Gligor, B. Bayrak, B. Ertek, Photoelectrocatalytic determination of NADH in a flow injection system with electropolymerized methylene blue, Electrochim. Acta. 56 (2011) 1138-1143. http://doi.org/10.1016/j.electacta.2010.10.084.

[13] J. L. Delaney, C. F. Hogan, J. Tian, W. Shen, Electrogenerated Chemiluminescence Detection in Paper-Based Microfluidic Sensors, Anal. Chem. 83 (2011) 1300-1306. http://doi.org/10.1021/ac102392t.

[14] S. Liu, Z. Du, P. Li, F. Li, Sensitive colorimetric visualization of dihydronicotinamide adenine dinucleotide based on anti-aggregation of gold nanoparticles via boronic acid – diol binding, Biosensors and Bioelectronics. 35 (2012) 443-446. http://doi.org/10.1016/j.bios.2012.02.040.

[15] K. C. Lin, Y. S. Li, S. M. Chen, Electrochemical determination of nicotinamide adenine dinucleotide and hydrogen peroxide based on poly(xanthurenic acid), flavin adenine dinucleotide and functionalized multi-walled carbon nanotubes,

Sensors and Actuators B: Chemical. 184 (2013) 212-219. http://doi.org/10.1016/j.snb.2013.04.081.

[16] P. Moozarm Nia, F. Lorestani, W. P. Meng, Y. Alias, A novel non-enzymatic H2O2 sensor based on polypyrrole nanofibers – silver nanoparticles decorated reduced graphene oxide nano composites, Appl. Surf. Sci. 332 (2015) 648-656. http://doi.org/10.1016/j.apsusc.2015.01.189.

[17] F. Ricci, A. Amine, G. Palleschi, D. Moscone, Prussian Blue based screen printed biosensors with improved characteristics of long-term lifetime and pH stability, Biosensors and Bioelectronics. 18 (2003) 165-174. http://doi.org/10.1016/S0956-5663(02)00169-0.

[18] V. K. Gupta, N. Atar, M. L. Yola, Z. Üstündağ, L. Uzun, A novel magnetic Fe@Au core – shell nanoparticles anchored graphene oxide recyclable nanocatalyst for the reduction of nitrophenol compounds, Water Res. 48 (2014) 210-217. http://doi.org/https://doi.org/10.1016/j.watres.2013.09.027.

[19] M. L. Yola, V. K. Gupta, T. Eren, A. E. Şen, N. Atar, A novel electro analytical nanosensor based on graphene oxide/silver nanoparticles for simultaneous determination of quercetin and morin, Electrochim. Acta. 120 (2014) 204-211. http://doi.org/10.1016/j.electacta.2013.12.086.

[20] B. Y. Wu, S. H. Hou, F. Yin, J. Li, Z. X. Zhao, J. D. Huang, Q. Chen, Amperometric glucose biosensor based on layer-by-layer assembly of multilayer films composed of chitosan, gold nanoparticles and glucose oxidase modified Pt electrode, Biosens. Bioelectron. 22 (2007) 838-844. http://doi.org/10.1016/j.bios.2006.03.009.

[21] Z. Wang, M. Li, P. Su, Y. Zhang, Y. Shen, D. Han, A. Ivaska, L. Niu, Direct electron transfer of horseradish peroxidase and its electrocatalysis based on carbon nanotube/thionine/gold composites, Electrochem. Commun. 10 (2008) 306-310. http://doi.org/10.1016/j.elecom.2007.12.011.

[22] H. Karimi-Maleh, F. Tahernejad-Javazmi, N. Atar, M. L. Yola, V. K. Gupta, A. A. Ensafi, A Novel DNA Biosensor Based on a Pencil Graphite Electrode Modified with Polypyrrole/Functionalized Multiwalled Carbon Nanotubes for Determination of 6-Mercaptopurine Anticancer Drug, Ind. Eng. Chem. Res. 54 (2015) 3634-3639. http://doi.org/10.1021/ie504438z.

[23] X. Huang, L. Zhang, Z. Zhang, S. Guo, H. Shang, Y. Li, J. Liu, Wearable biofuel cells based on the classification of enzyme for high power outputs and lifetimes, Biosensors and Bioelectronics. 124-125 (2019) 40-52. http://doi.org/10.1016/j.bios.2018.09.086.

[24] J. Liu, L. Zhang, C. Fu, Os-complex-based amperometric bienzyme biosensor for continuous determination of lactate in saliva, Anal. Methods-UK. 7 (2015) 6158-6164. http://doi.org/10.1039/c5ay01110h.

[25] J. Liu, S. Sun, H. Shang, J. Lai, L. Zhang, Electrochemical Biosensor Based on Bienzyme and Carbon Nanotubes Incorporated into an Os‐complex Thin Film for Continuous Glucose Detection in Human Saliva, Electroanal. 28 (2016) 2016-2021. http://doi.org/10.1002/elan.201501179.

[26] W. Jia, G. Valdes-Ramirez, A. J. Bandodkar, J. R. Windmiller, J. Wang, Epidermal biofuel cells: energy harvesting from human perspiration, Angew Chem Int Ed Engl. 52 (2013) 7233-7236. http://doi.org/10.1002/anie.201302922.

[27] L. Qian, X. Yang, Composite film of carbon nanotubes and chitosan for preparation of amperometric hydrogen peroxide biosensor, Talanta. 68 (2006) 721-727. http://doi.org/10.1016/j.talanta.2005.05.030.

[28] Y. Zhao, W. Zhang, H. Chen, Q. Luo, S. F. Y. Li, Direct electrochemistry of horseradish peroxidase at carbon nanotube powder microelectrode, Sensors & Actuators: B. Chemical. 87 (2002) 168-172. http://doi.org/10.1016/S0925-4005(02)00232-0.

[29] Y. Chen, Y. Li, D. Sun, D. Tian, J. Zhang, J. Zhu, Fabrication of gold nanoparticles on bilayer graphene for glucose electrochemical biosensing, Journal of Materials Chemistry. 21 (2011) 7604. http://doi.org/10.1039/c1jm10293a.

[30] Y. Zhang, R. Yuan, Y. Chai, Y. Xiang, C. Hong, X. Ran, An amperometric hydrogen peroxide biosensor based on the immobilization of HRP on multi-walled carbon nanotubes/electro-copolymerized nano-Pt-poly(neutral red)

composite membrane, Biochem. Eng. J. 51 (2010) 102-109. http://doi.org/10.1016/j.bej.2010.06.001.

[31] K. Zhou, Y. Zhu, X. Yang, J. Luo, C. Li, S. Luan, A novel hydrogen peroxide biosensor based on Au – graphene – HRP – chitosan biocomposites, Electrochim. Acta. 55 (2010) 3055-3060. http://doi.org/10.1016/j.electacta.2010.01.035.

[32] C. Xiang, Y. Zou, L. Sun, F. Xu, Direct electrochemistry and enhanced electrocatalysis of horseradish peroxidase based on flowerlike ZnO – gold nanoparticle – Nafion nanocomposite, Sensors and Actuators B: Chemical. 136 (2009) 158-162. http://doi.org/https://doi.org/10.1016/j.snb.2008.10.058.

[33] X. Zhao, Z. Mai, X. Kang, X. Zou, Direct electrochemistry and electrocatalysis of horseradish peroxidase based on clay-chitosan-gold nanoparticle nanocomposite, Biosens. Bioelectron. 23 (2008) 1032-1038. http://doi.org/10.1016/j.bios.2007.10.012.

[34] K. Guo, K. Qian, S. Zhang, J. Kong, C. Yu, B. Liu, Bio-electrocatalysis of NADH and ethanol based on graphene sheets modified electrodes, Talanta. 85 (2011) 1174-1179. http://doi.org/10.1016/j.talanta.2011.05.038.

[35] M. Zhou, Y. Zhai, S. Dong, Electrochemical Sensing and Biosensing Platform Based on Chemically Reduced Graphene Oxide, Anal. Chem. 81 (2009) 5603-5613. http://doi.org/10.1021/ac900136z.

[36] X. Liu, B. Li, M. Ma, G. Zhan, C. Liu, C. Li, Amperometric sensing of NADH and ethanol using a hybrid film electrode modified with electrochemically fabricated zirconia nanotubes and poly (acid fuchsin), Microchim. Acta. 176 (2012) 123-129. http://doi.org/10.1007/s00604-011-0701-5.

[37] F. Ricci, A. Amine, D. Moscone, G. Palleschi, A probe for NADH and H2O2 amperometric detection at low applied potential for oxidase and dehydrogenase based biosensor applications, Biosensors and Bioelectronics. 22 (2007) 854-862. http://doi.org/10.1016/j.bios.2006.03.004.

[38] G. P. Keeley, A. O'Neill, M. Holzinger, S. Cosnier, J. N. Coleman, G. S. Duesberg, DMF-exfoliated graphene for electrochemical NADH detection, Phys. Chem. Chem. Phys. 13 (2011) 7747-7750. http://doi.org/10.1039/c1cp20060g.

[39] C. Chen, Y. Chen, M. Lin, Amperometric determination of NADH with Co3O4 nanosheet modifiedelectrode, Biosensors and Bioelectronics. 42 (2013) 379-384. http://doi.org/10.1016/j.bios.2012.10.086.

[40] M. Wooten, W. Gorski, Facilitation of NADH Electro-oxidation at Treated Carbon Nanotubes, Anal. Chem. 82 (2010) 1299-1304. http://doi.org/10.1021/ac902301b.

Figure and Table Legends

Fig. 1. Schematic diagram of detecting NADH by the biosensor.

Fig. 2. SEM images (A) CNTs and (B) CNTs/TTF composite electrodes.

Fig. 3. (A) EIS of various modified electrodes. Bare GC (a), GC/CNTs (b), GC/CNTs/TTF (c) and GC/CNTs/HRP (d). The Randles equivalent circuit used to fit the EIS data. (B) CV curves of various modified electrodes in 0.1 M PBS solution saturated with N_2. GC/CNTs (a), GC/CNTs/TTF (b) and GC/CNTs/TTF/HRP (c). The potential scan rate was 100 mV s^{-1}. (C) CV curves of GC/CNTs/TTF/HRP electrode at different scan rates: 10 mV s^{-1} (a), 20 mV s^{-1} (b), 30 mV s^{-1} (c), 40 mV s^{-1} (d), 50 mV s^{-1} (e), 60 mV s^{-1} (f), 70 mV s^{-1} (g), 80 mV s^{-1} (h), 90 mV s^{-1} (i) and 100 mV s^{-1} (j). (D) Plot of the relationship between redox peak current densities and scan rates from 1 mV s^{-1} to 100 mV s^{-1}. All CV curves were run in the PBS solution saturated with N_2.

Fig. 4. (A) CV curves of GC/CNTs/TTF/HRP electrode in the PBS solution with different concentration of H_2O_2: 0mM (a), 1mM (b), 5mM (c) and 10mM (d). The scan rate was 100 mV s^{-1}. (B) Amperometric i–t curve of the biosensor by successivly adding different concentration of H_2O_2 to the PBS solution. Operating potential: -0.3 V. (C) Calibration curve between current and the concentration of H_2O_2.

Fig. 5. (A) CV curves of CNTs/TTF/HRP modified H_2O_2 biosensor in the PBS buffer containing MB with different concentration of NADH: 0mM (a), 0.1mM (b), 0.3mM (c) and 0.6mM (d). The scan rate was 100 mV s^{-1}. (B) Amperometric i-t curve of the CNTs/TTF/HRP modified H_2O_2 biosensor by successively adding different concentration of NADH to the base solution. Operating potential: -0.3 V. (C) Calibration curve between current and the concentration of NADH. (D) Amperometric response of the CNTs/TTF/HRP modified H_2O_2 biosensor with the subsequent addition UA, glucose and NADH.

Table 1. Comparison of GC/CNTs/TTF/HRP electrode with other amperometric NADH biosensors.

Table 1.
Comparison of GC/CNTs/TTF/HRP electrode with other amperometric NADH biosensors.

Working electrode	Potential (V)	Linear range (μM)	Limit of detection (μM)	Reference
Au(111)/MB/graphene	0.74 (*vs.* Ag/AgCl)	1-264	0.3	[3]
GC/CNTs/FAD [1]/polyXa [2]	0.15 (*vs.* Ag/AgCl)	5-170	1	[15]
GC/graphene	0.5 (*vs.* SCE [10])	50-1400	20	[34]
GC/CR-GO [3]	0.45 (*vs.* Ag/AgCl)	40-800	10	[35]
GC/PAF [4]/nano−ZrO_2 [5]	0.4 (*vs.* SCE)	1-100	1	[36]
SPEs [6]/PB [7]	– 0.05 (*vs.* Ag/AgCl)	1-100	0.5	[37]
GC/GNS [8]	0.4 (*vs.* Ag/AgCl)	45-360	15	[38]
carbon ink/Co_3O_4 nanosheet [9]	0.1 (*vs.* Ag/AgCl)	10-100	4.25	[39]
GC/chitosan/CNTs	– 0.05 (*vs.* Ag/AgCl)	10-100	4	[40]
GC/CNTs/TTF/HRP	– 0.3 (*vs.* Ag/AgCl)	10-790	1.53	this work

[1] Flavin adenine dinucleotide
[2] Poly xanthurenic acid
[3] Chemically reduced graphene oxide
[4] Poly (acid fuchsin)
[5] Zirconia nanotubes
[6] Screen-printed electrodes
[7] Prussian blue
[8] Graphite nanosheet
[9] Cobalt oxide nanosheet
[10] Saturated calomel electrode

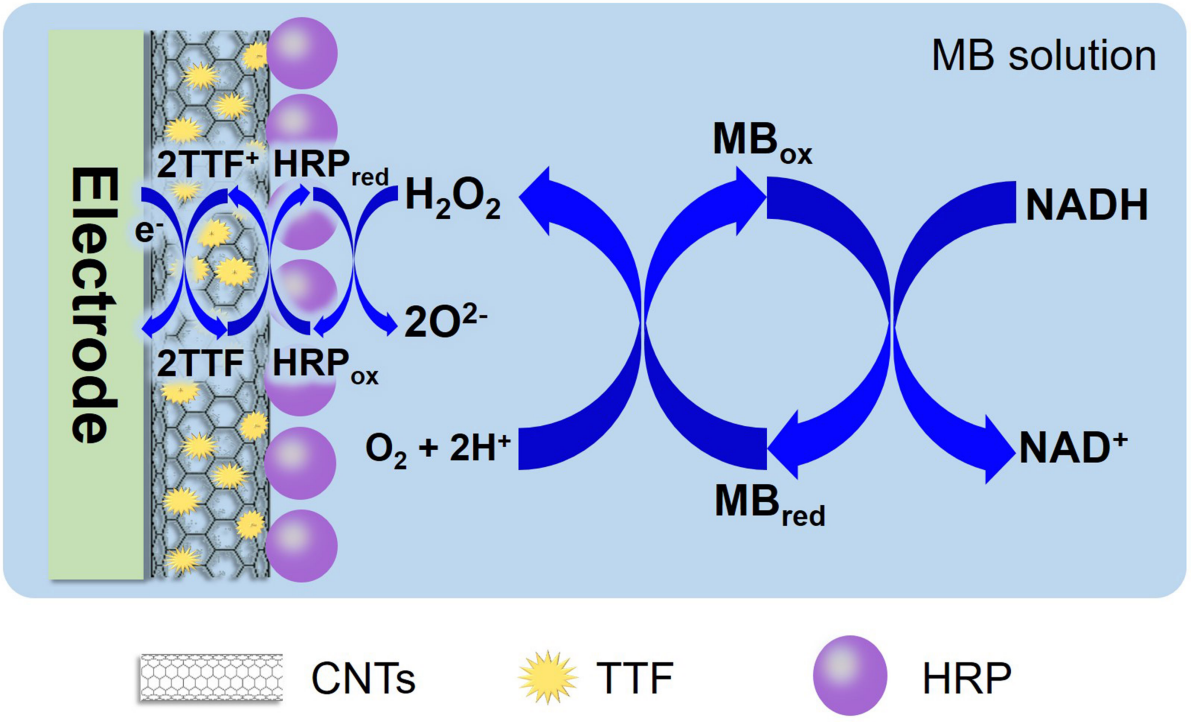

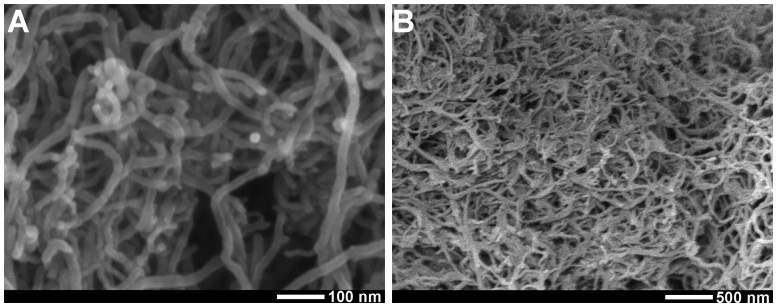

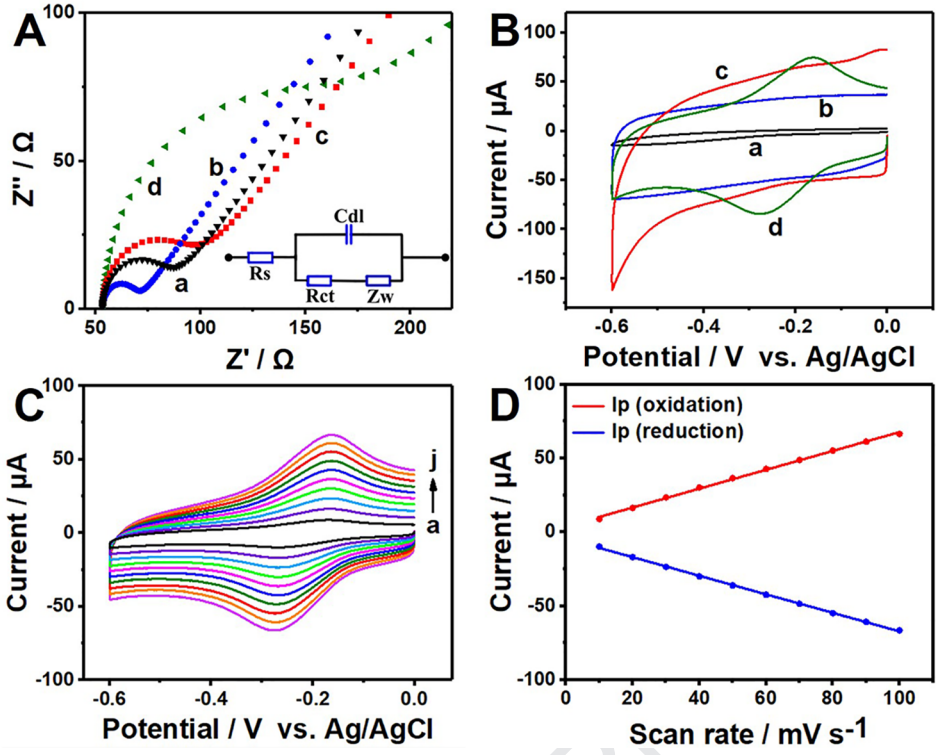

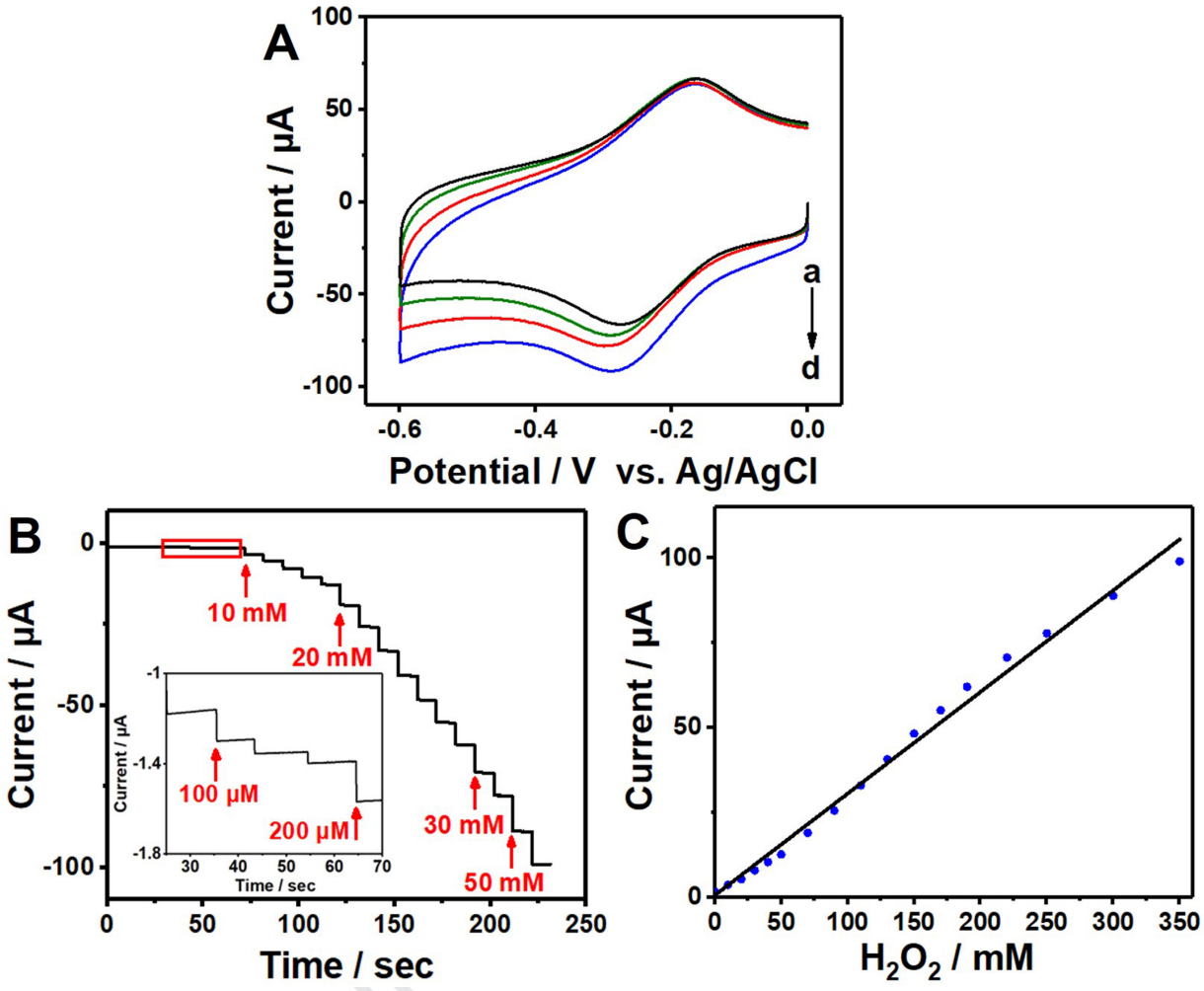
A
Current / μA
Potential / V vs. Ag/AgCl
a
d
B
Current / μA
Time / sec
10 mM
20 mM
30 mM
50 mM
100 μM
200 μM
C
Current / μA
H2O2 / mM

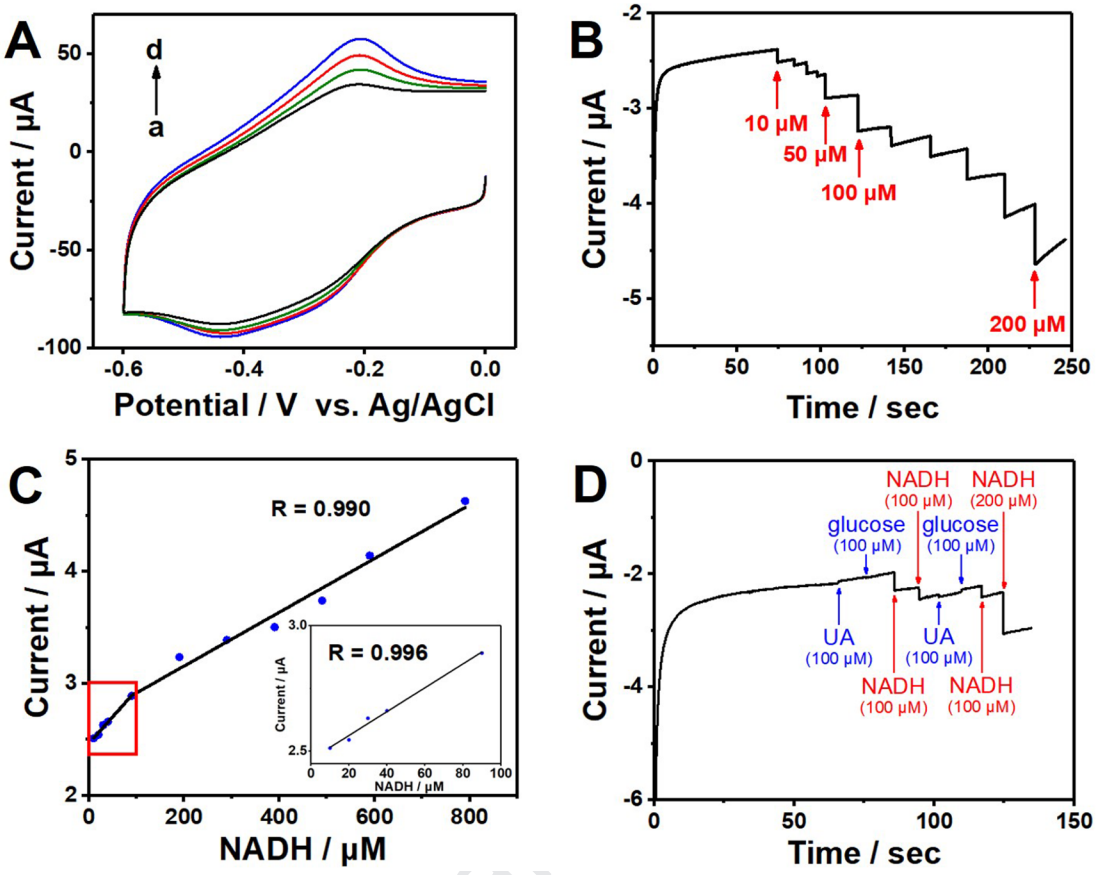
A
d
a
Current / μA
Potential / V vs. Ag/AgCl
B
10 μM
50 μM
100 μM
200 μM
Current / μA
Time / sec
C
R = 0.990
R = 0.996
Current / μA
NADH / μM
D
NADH (100 μM)
NADH (200 μM)
glucose (100 μM)
glucose (100 μM)
UA (100 μM)
UA (100 μM)
NADH (100 μM)
NADH (100 μM)
Current / μA
Time / sec

Highlight

- Detecting the NADH in the buffer containing methylene blue through a H_2O_2 biosensor modified with carbon nanotubes (CNTs)/tetrathiafulvalene (TTF)/horseradish peroxidase (HRP) sensitive thin film in the buffer containing methylene blue.

- Wide linear range, high sensitivity and low detection limit for determining NADH.

- A low operating potential of – 0.3 V (vs. Ag/AgCl) with excellent selectivity and anti-interference ability.